POLITECNICO DI TORINO
Repository ISTITUZIONALE

Improving the Performance of PVDF/PVDF- g-PEGMA Ultrafiltration Membranes by Partial Solvent Substitution with Green Solvent Dimethyl Sulfoxide during Fabrication

Original
Improving the Performance of PVDF/PVDF- g-PEGMA Ultrafiltration Membranes by Partial Solvent Substitution with Green Solvent Dimethyl Sulfoxide during Fabrication / Wu, Q.; Tiraferri, A.; Wu, H.; Xie, W.; Liu, B.. - In: ACS OMEGA. - ISSN 2470-1343. - 4:22(2019), pp. 19799-19807. [10.1021/acsomega.9b02674]

Availability:
This version is available at: 11583/2779232 since: 2020-01-10T17:31:45Z

Publisher:
American Chemical Society

Published
DOI:10.1021/acsomega.9b02674

Terms of use:

This article is made available under terms and conditions as specified in the corresponding bibliographic description in the repository

Publisher copyright

(Article begins on next page)

19 April 2024

This is an open access article published under an ACS AuthorChoice License, which permits copying and redistribution of the article or any adaptations for non-commercial purposes.

ACS OMEGA

Article

Cite This: ACS Omega 2019, 4, 19799−19807

http://pubs.acs.org/journal/acsodf

Improving the Performance of PVDF/PVDF-*g*-PEGMA Ultrafiltration Membranes by Partial Solvent Substitution with Green Solvent Dimethyl Sulfoxide during Fabrication

Qidong Wu,[†] Alberto Tiraferri,[‡] Haibo Wu,[†] Wancen Xie,[†] and Baicang Liu*[,†]

[†]College of Architecture and Environment, Institute of New Energy and Low-Carbon Technology, Institute for Disaster Management and Reconstruction, Sichuan University, Chengdu, Sichuan 610207, P. R. China

[‡]Department of Environment, Land and Infrastructure Engineering, Politecnico di Torino, Corso Duca degli Abruzzi 24, 10129 Turin, Italy

Supporting Information

ABSTRACT: Traditional organic solvents used in membrane manufacturing, such as dimethylformamide and tetrahydrofuran, are generally very hazardous and harmful to the environment and human health. Their total or partial substitution with green solvent dimethyl sulfoxide (DMSO) is proposed to fabricate membranes composed of poly(vinylidene fluoride) (PVDF) blended with PVDF-*graft*-poly(ethylene glycol) methyl ether methacrylate (PEGMA), with the purpose to accomplish a greener chemical process and enhance the membrane performance. Various organic solvent compositions were first investigated using the Hansen solubility theory, and the best mixture was thus applied experimentally. The membrane prepared by a ratio of *N*,*N*-dimethylacetamide/DMSO = 7:3 outperformed the membranes prepared by other solvent mixtures. This membrane showed high wetting behavior with the water contact angle declining from 71 to 7° in 18 s and a pure water flux reaching values larger than 700 L m^{-2} h^{-1} under 0.07 MPa applied hydraulic pressure. The membrane rejected sodium alginate at a rate of 87%, and nearly complete flux recovery was achieved following fouling and physical cleaning. The introduction of green chemistry concepts to PVDF/PVDF-*g*-PEGMA blended membranes is a step forward in the goal to increase the sustainability of membrane production.

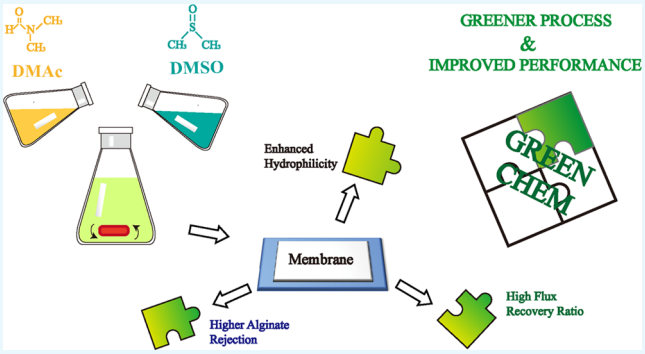

1. INTRODUCTION

Poly(vinylidene) fluoride (PVDF) is a well-established polymeric material to produce ultrafiltration (UF) and microfiltration (MF) membranes owing to its exceptional mechanical properties, chemical resistance, and thermal stability.[1−7] However, despite its many advantages, the hydrophobicity of PVDF can induce severe membrane fouling, which is a main obstacle that limits its applications.[8−12] Thanks to the compatibility of the PVDF matrix with amphiphilic copolymers, modifications of PVDF membranes by blending with other more hydrophilic components have been reported widely.[13−17] The atom transfer radical polymerization (ATRP) method can be applied to enhance the properties of polymers by grafting chains with different characteristics, making the preparation of many new copolymers possible.[18−25] Specifically, PVDF-*graft*-poly(ethylene glycol) methyl ether methacrylate (PVDF-*g*-PEGMA) has been successfully synthesized and characterized.[20,26,27] Membranes with promising fouling resistance behavior were thus produced by blending this PVDF-*g*-PEGMA material with traditional PVDF.[28]

Liu et al. fabricated high-performance and detect-free membranes consisting of PVDF blended with PVDF-*g*-PEGMA with a unique periodic nodular structure.[28] The membrane exhibited a high sodium alginate (SA) rejection and a very high water permeance of 5170 L m^{-2} h^{-1} bar^{-1}, roughly 1 magnitude higher than that obtained by Hashim et al. or achieved by commercial membranes.[29] Chen et al. further explored the formation mechanism of the periodic nodular structure, and they found that the structure can only be obtained when PVDF-*g*-PEGMA and 1-methyl-2-pyrrolidinone (NMP) are deployed in the casting solution.[30] Wang et al. investigated the properties of membranes fabricated using PVDF-*g*-PEGMA obtained by different synthesis reaction times and found that the membrane pore size distribution of the final membrane is a function of this parameter.[31] Wang et al. also incorporated nonwoven poly(ethylene terephthalate) (PET) fabrics as a support layer to enhance the mechanical

Received: August 19, 2019
Accepted: October 24, 2019
Published: November 7, 2019

Downloaded via POLITECNICO DI TORINO on January 10, 2020 at 16:30:28 (UTC).
See https://pubs.acs.org/sharingguidelines for options on how to legitimately share published articles.

© 2019 American Chemical Society

DOI: 10.1021/acsomega.9b02674
ACS Omega 2019, 4, 19799−19807

Table 1. Compositions and Viscosities of the Casting Solutions

membrane ID	PVDF (g)	DMAc (g)	DMSO (g)	NMP (g)	THF (g)	DMF (g)	PVDF-*g*-PEGMA (g)	PVDF-*g*-PEGMA/PVDF (w/w %)	viscosity (mPa·s, 25 °C)
PVDF1-DMSO	12.0		86.2				1.8	15	834
PVDF2-DMAc and DMSO[a]	12.0	60.3	25.9				1.8	15	595
PVDF3-DMSO and NMP[b]	12.0		43.1	43.1			1.8	15	775
PVDF4-DMSO, THF, and DMF[c]	12.0		43.1		12.9	30.2	1.8	15	523

[a]The casting solution of PVDF2 contains 70% DMAc and 30% DMSO. [b]The casting solution of PVDF3 contains 50% DMSO and 50% NMP. [c]The casting solution of PVDF4 contains 50% DMSO, 15% THF, and 35% DMF.

properties of the fabricated PVDF blended PVDF-*g*-PEGMA ultrafiltration membrane and to increase the resistance to a pressure up to 23.3 MPa, thus satisfying the requirements for industrial applications.[8]

Previous studies were mainly focused on the performance of the blended PVDF-based membranes. There, and in the vast majority of the membrane fabrication studies, the hazards intrinsic in the use of the traditional solvent have been neglected. Traditional organic solvents are toxic and hazardous. For example, dimethylformamide (DMF), a flammable liquid, is dangerous if inhaled or exposed to skin and may cause fertility problems. The concepts of green chemistry have been proposed for some time and have developed rapidly.[32−34] The objectives of green chemistry are to decrease the production and use of hazardous substances and reduce the energy consumption, moving toward renewable sources.[32,34,35] Anastas and Werner proposed 12 principles of green chemistry[36] with the main goal to prevent contaminations at the very beginning of the production stage.[32,33] In the membrane manufacturing process, solvents play a critical part in determining the properties of the membrane by influencing the solvent−nonsolvent and solvent−polymer interactions. Switching toward greener solvents while maintaining or improving the membrane performance is far from a trivial task.[34,37−39] Nevertheless, green solvents should be used for membrane fabrication to reduce the impact and to facilitate the operation of this industrial process, especially considering that the ultimate goal of many membrane applications is precisely the removal of contaminations from liquid streams.[40,41] Solvent dimethyl sulfoxide (DMSO) is a green solvent that is nontoxic and more easily recyclable compared to traditional solvents.[42−44]

Based on the concept of green chemistry and on our previous studies on PVDF-based membranes, we optimize the fabrication of membranes composed of PVDF blended with PVDF-*g*-PEGMA by substituting traditional solvents, e.g., tetrahydrofuran (THF), DMF, and NMP, with DMSO. The optimal partial substitution is estimated using the Hansen solubility theory to investigate quantitatively the polymer−solvent interaction and to ensure the compatibility between solvents and polymers.[45] We thus fabricate membranes using the promising solvent mixtures, and we evaluate the performance and the characteristics of the membranes under ultrafiltration conditions. The goal of this study is to fabricate a membrane with desired structural properties and high performance in terms of both productivity and removal of organic macromolecules using a greener synthesis route.

2. MATERIALS AND METHODS

2.1. Chemicals and Materials. PVDF (average M_w = 534 K), PEGMA (M_n = 500 g mol^{-1}), 4-4′-dimethyl-2-2′-dipyridyl (DMDP, 99.5%), NMP (anhydrous, 99.5%), silicone oil, DMF (99.8%), DMSO (99.9%), THF (≥99.9%), copper(I) chloride (CuCl, trace metals basis, ≥99.995%), *N*,*N*-dimethylacetamide (DMAc, Reagent Plus, 99%), NaCl (ACS reagent, ≥99.0%), and sodium alginate (SA, Halal grade) were purchased from MilliporeSigma (St. Louis, Missouri). Deionized water (DI water) was produced using an ultrapure water system purchased from Ulupure (Chengdu, China).

2.2. Procedure to Synthesize the Graft Copolymer PVDF-*g*-PEGMA. The procedure to synthesize the PVDF-*g*-PEGMA copolymer was conducted as follows:[28,31] 5 g of PVDF was dissolved in 40 mL of NMP at 50 °C in a conical flask while stirring. Then, 50 mL of PEGMA, 0.23 g of DMDP, and 0.04 g of CuCl were added to the same conical flask, which had already been cooled to room temperature. Right after this addition, the reaction mixture was stirred at 200 rpm and bubbled using nitrogen gas for 30 min. The flask was sealed using a rubber septum to prevent air oxygen from disturbing the ATRP.[24] Then, a silicon oil bath was used to heat the conical flask to 90 °C. The high-temperature reaction lasted for 19 h with stirring. Finally, the resulting copolymer mixture was sealed and stored at room temperature.[31]

2.3. Calculation of the Hanson Solubility Parameter. According to the Hansen solubility theory, the affinity between the solvent and polymer can be analyzed quantitatively. δ_t, the total solubility parameter, is the combination of three parameters: δ_d, δ_h, and δ_p, which quantitatively represent the dispersion parameter (δ_d), the hydrogen bonding parameter (δ_h), and the polar parameter (δ_p), respectively. δ_d, δ_h, and δ_p can be calculated using the following equations.[46]

$$\delta_t^2 = \delta_d^2 + \delta_p^2 + \delta_h^2 \quad (1)$$

$$\delta_d = \sum F_{di}/V \quad (2)$$

$$\delta_h = \sqrt{\sum E_{hi}/V} \quad (3)$$

$$\delta_p = \sqrt{\sum F_{pi}^2}/V \quad (4)$$

where F_{di} is the group contribution to the dispersion component. The parameter E_{hi} represents the hydrogen bonding energy for each structure group. The F_{pi} parameter is the group contribution to the polar force component. For mixed solvents, such as binary mixed solvents, δ_d, δ_h, and δ_p can be calculated using the volume fraction for each solvent by applying the following equation

DOI: 10.1021/acsomega.9b02674
ACS Omega 2019, 4, 19799−19807

$$(\text{Volume}\cdot\text{fraction})_{\text{solventA}} = \frac{\left(\frac{W_t\cdot\text{fraction}}{\text{density}}\right)_{\text{solventA}}}{\left(\frac{W_t\cdot\text{fraction}}{\text{density}}\right)_{\text{solventA}} + \left(\frac{W_t\cdot\text{fraction}}{\text{density}}\right)_{\text{solventB}}} \quad (5)$$

Application of the mixing law allows calculation of the solubility parameters of mixed solvents as

$$\delta_d = (\text{volume}\cdot\text{fraction})_A \times \delta_{dA} + (\text{volume}\cdot\text{fraction})_B \times \delta_{dB} \quad (6)$$

$$\delta_p = (\text{volume}\cdot\text{fraction})_A \times \delta_{pA} + (\text{volume}\cdot\text{fraction})_B \times \delta_{pB} \quad (7)$$

$$\delta_h = (\text{volume}\cdot\text{fraction})_A \times \delta_{hA} + (\text{volume}\cdot\text{fraction})_B \times \delta_{hB} \quad (8)$$

The ternary mixed solvents can be calculated using the analogous methodology for three components. The affinity between the polymer and solvents can be represented by the value of R_a, which was calculated as follows

$$R_a = \sqrt{4(\delta_{d1} - \delta_{d2})^2 + (\delta_{p1} - \delta_{p2})^2 + (\delta_{h1} - \delta_{h2})^2} \quad (9)$$

The detailed calculations of the solvents used in the experiments can be found in the Supporting Information (SI).

2.4. Membrane Casting. Table 1 lists the compositions of casting solutions used for membrane synthesis in this study. All of the membranes were synthesized at a constant room temperature of 25 °C and ∼45% humidity, controlled by an air conditioner. The casting solutions were added to a conical flask and then heated to 60 °C while stirring at 500 rpm. After the copolymer and PVDF powder were dissolved completely, the solution was degassed for at least 2 h before casting. Next, the solution was cast using an 8 in.-wide doctor blade (Universal blade applicator, Paul N. Gardner Company, Inc., Pompano Beach, FL) on a first-grade surface optical glass; the gate height of the blade was set to be 200 μm. Then, the glass was immersed in a bath that contained deionized water at room temperature (25 °C). After 48 h, some of the cast membranes were air-dried for 24 h for further investigation and the others were kept in DI water at 4 °C for further experiments.

2.5. Model Foulant. The antifouling performance of the membranes was evaluated using a model extracellular polymeric substance, namely, sodium alginate (SA). The SA stock solution of 2 g L^{-1} was prepared in deionized water and stored at 4 °C. In this experiment, the UV−vis spectrometer (Thermo Orion Aquamate 8000) was used to determine the concentrations of SA with a fixed wavelength of 220 nm.[47,48]

2.6. Membrane Characterizations. The elemental surface composition of the membrane for a depth within 5 nm was analyzed using X-ray photoelectron spectroscopy (XPS, Axis Ultra, Kratos Analytical Ltd., U.K.). The spectra with 1 eV scan resolution were obtained by sweeping over the electron binding energy range of 0−1200 eV; then, the atomic concentrations of the corresponding elements were calculated from peak areas following high-resolution scans with 0.1 eV resolution. The spectra of Fourier transform infrared attenuated total reflectance (FTIR-ATR, Alpha, Bruker) were obtained by collecting over the 650−4000 cm^{-1} wavenumber range with 64 scans of 2 cm^{-1} resolution. The membrane morphology was observed using field-emission scanning electron microscopy (FESEM, JSM-7500F, JEOL Ltd., Tokyo, Japan). To observe the cross-sectional morphology, the samples were frozen using liquid nitrogen for 3 min before brittle fracture. The membrane samples were first fixed on stubs using carbon tape and then sputter-coated with a gold layer of ∼2 nm (Q150R-ES, Quorum, U.K.). The images were taken under a 5 kV accelerating voltage with different magnifications. The thickness of the membranes was measured using an electronic digital micrometer (Marathon Watch Company Ltd., Canada).

The contact angles of the blended membranes were measured using the KRÜSS DSA 25S measuring apparatus (KRÜSS GmbH, Germany). For each measurement, DI water droplets (2 μL) were placed on the sample surface to obtain the dynamic variations of the contact angle for a time period of 18 s, starting from the instant when the droplet was placed on the sample. The experiment was repeated at different locations on the membrane for about 10 spots. Atomic force microscopy (AFM, Multimode 8, Bruker, Germany) was used to obtain the surface roughness. In this test, a resonant frequency of 0.997 kHz was used to scan the membranes on 5 μm × 5 μm size areas at least 2 times. The viscosity of the casting solutions was measured by a rotary viscometer (NDJ-79, Changji Geological Instrument Co. Ltd., Shanghai) using 10 mL casting solution samples at 25 °C. The mechanical properties of the fabricated membranes were measured by an electronic single fiber strength meter (Yuanmao Instrument Co. Ltd., Laizhou, China). This experiment was repeated at least 10 times using samples with a length of 10 mm and an operational speed of 10 mm min^{-1}. The maximum and minimum values of the tensile strength were discarded, and the average value was then calculated. The detailed mechanical performance of the fabricated membranes can be found in the SI.

A dead-end filtration cell (Amicon 8200, Millipore) was used to measure the permeability and the antifouling performance of the membranes. The membranes were cut into circular samples with an effective area of 28.7 cm^2. The filtration cell (200 mL) was connected to a dispensing vessel (5 L). The permeate stream was recorded every minute. All of the experiments were performed at room temperature, and nitrogen gas was used to maintain a constant pressure of 0.07 MPa (10 psi). For each pure water filtration or antifouling experiment, the duration of the flux measurement was the lesser one between a predetermined time or the time needed to filter 4 L of feed water. First, the membrane sample was compacted using 4 L of water for 2 h, while the flux of permeate water was recorded as J_{w1} (L m^{-2} h^{-1}). Second, a conditioning period of the membrane followed using 4 L of NaCl solution of 10 mM L^{-1} as a feed for 2 h. Third, the model fouling test was conducted using 4 L of feed solution that contained 20 mg L^{-1} SA and 10 mmol L^{-1} NaCl for 5 h. During the fouling test, the concentration polarization was minimized using a stirring plate (PC-420D, Corning) adjusted to 200 rpm, on which the filtration cell was placed. The flux was recorded as J_p (L m^{-2} h^{-1}). Finally, the membrane was physically cleaned using a constant DI water flow of 2.7 L min^{-1} for 1 min, maintaining the water surface 25 cm above the membrane surface. After cleaning, the recovery flux, J_{w2} (L m^{-2} h^{-1}), was measured using water as feed solution for 1 h. The flux recovery ratio (FRR), total flux decline ratio (DR_t), reversible flux decline ratio (DR_r), and irreversible flux decline ratio (DR_{ir}) were calculated by the following equations using an average value from three tests.[18,49,50]

DOI: 10.1021/acsomega.9b02674
ACS Omega 2019, 4, 19799−19807

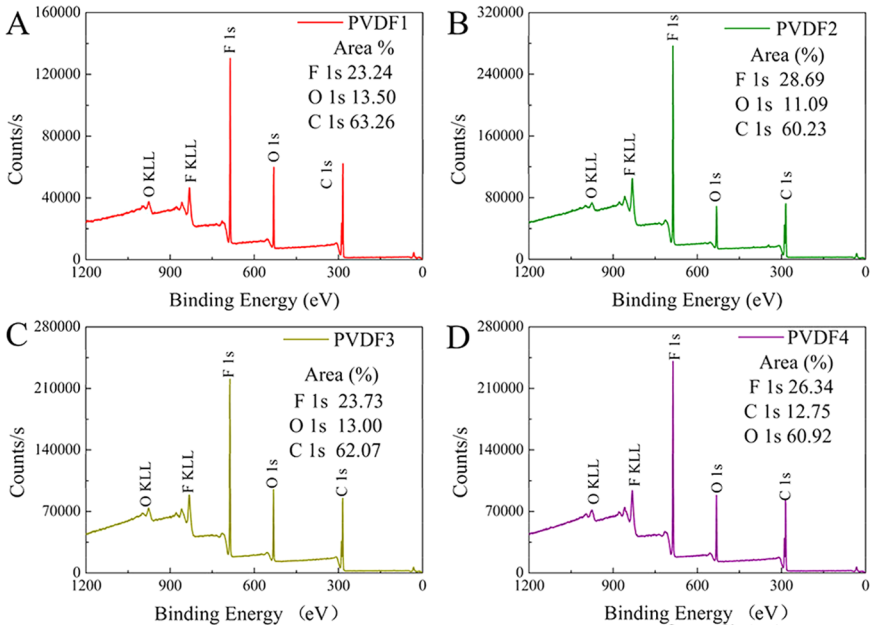

Figure 1. XPS spectra of the PVDF/PVDF-*g*-PEGMA membranes cast from different solvents or solvent mixtures: (a) PVDF1, DMSO; (b) PVDF2, DMSO/DMAc = 3:7; (c) PVDF3, DMSO/NMP = 5:5; and (d) PVDF4, DMSO/THF/DMF = 5:1.5:3.5. The content of the main elements was calculated and reported in the graphs.

Table 2. Performance of PVDF/PVDF-*g*-PEGMA Fabricated in Previous Studies

membrane ID	element composition (C/O/F) (%)	D_{avg} (nm)	D_{max} (nm)	roughness (nm)	DI permeability (L m^{-2} h^{-1} bar^{-1})	SA rejection (%)	FRR (%)	CA variation (deg)
JMS7[28a]	55.8/6.73/37.4	31	183	15.3	5170	87.19	39	73−61° (200 s)
19H[31b]	52.05/12.89/35.06	18	59	30.7	1068	73.3	70.8	73−33° (180 s)
b[30]	57.72/6.37/35.91	34 ± 19	126	27.5	374	87	36	70−67° (60 s)
d[30c]	56.63/6.49/36.89	42 ± 23	146	32.7	949	94	47	74−72° (60 s)
f[30c]	57.83/4.67/37.5	15 ± 5	49	26.3				74−73° (60 s)
M0[8]				55.8	232	47	60	
M1[8d]		51 ± 4	118	19.0	929	44	82	100−92° (180 s)
M2[8d]		47 ± 3	95	14.2	800	50	87	69−20° (35 s)

[a]The membranes were all fabricated using casting solution contains 18% PVDF and 15% wt PVDF-*g*-PEGMA. The solvent in casting solution was THF/DMF = 3:7 unless stated. [b]The solvent in casting solution was DMF. [c]The solvent in casting solution was NMP. [d]M1 and M2 had PET support layers, M1 with a thin layer of 29 nm and M2 was 84 nm.

$$\mathrm{FRR} = \frac{J_{w2}}{J_{w1}} \times 100\% \quad (10)$$

$$\mathrm{DR_t} = \left(1 - \frac{J_p}{J_{w1}}\right) \times 100\% \quad (11)$$

$$\mathrm{DR_r} = \left(\frac{J_{w2} - J_p}{J_{w1}}\right) \times 100\% \quad (12)$$

$$\mathrm{DR_{ir}} = \left(\frac{J_{w1} - J_{w2}}{J_{w1}}\right) \times 100\% \quad (13)$$

3. RESULTS AND DISCUSSION

3.1. Elemental Composition of the Membranes. XPS results of all of the PVDF/PVDF-*g*-PEGMA membranes are displayed in Figure 1. The membrane was synthesized using a PVDF/PVDF-*g*-PEGMA mixture dissolved in different organic solvents or solvent mixtures. The composition percentage of the three main elements was within a small range, with oxygen ~12.6%, carbon ~61.4%, and fluorine ~25.5%. Because the organic solvents and the unreacted PEGMA diffused out from the polymer film and into water during phase separation, the only source of oxygen in the samples was the PEGMA segments in the PVDF-*g*-PEGMA chains. The appearance of oxygen in the spectra, besides carbon and fluorine, reflects that the amphiphilic PEGMA segments in the PVDF-*g*-PEGMA migrated preferentially to the membrane surface, indicating the successful blending of PVDF-*g*-PEGMA with PVDF in different casting solutions.[31] As listed in Table 2, compared with other membranes cast previously from PVDF blended with PVDF-*g*-PEGMA, the content of carbon and oxygen was higher, while that of fluorine was lower.[8,28,30,31] This observation is explained with the smaller proportion of PVDF in the blend and the larger amount of PEGMA segments that migrated to the membrane surface. The viscosity might be an important factor affecting the migration of PEGMA segments to the membrane surface in this study.[31] A lower viscosity weakened the exchange barrier between the nonsolvent and solvent, which accelerated the phase inversion. Therefore, the migration of PEGMA segments to the membrane surface could be more effective. The existence of

DOI: 10.1021/acsomega.9b02674
ACS Omega 2019, 4, 19799−19807

more PEGMA segments may improve some properties of the membranes. For example, it may decrease the surface tension and polarity to increase the hydrophilicity of the membrane; thus, potentially, the antifouling property of the membrane increased.

3.2. ATR-FTIR Spectra. Figure 2 shows the ATR-FTIR spectra of PVDF/PVDF-*g*-PEGMA membranes. The 1727 cm^{-1} band represents the C═O stretching band, while the 1638 cm^{-1} band represents the C═C stretching band.[17,30,51] The existence of C═O bonds indicates that the PEGMA segments were present in all of the membrane surfaces, while the absence of C═C implies that the unreacted PEGMA was removed during phase separation by diffusing out into the coagulation bath. This result suggests that PEGMA was successfully grafted onto PVDF because the synthesized PVDF-*g*-PEGMA contains only C═O bonds and no C═C bonds.

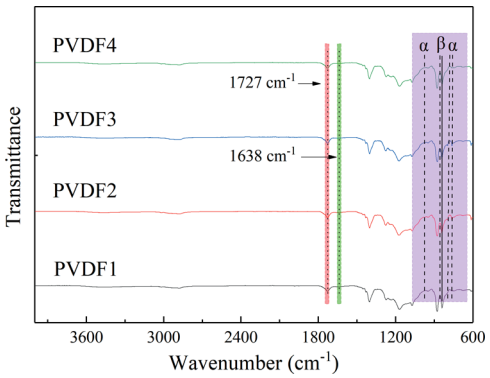

Figure 2. ATR-FTIR spectra of the PVDF/PVDF-*g*-PEGMA membranes cast using different solvents or solvent mixtures. PVDF1, DMSO; PVDF2, DMSO/DMAc = 3:7, PVDF3, DMSO/NMP = 5:5; and PVDF4, DMSO/THF/DMF = 5:1.5:3.5. The 1727 cm^{-1} peak represents C═O bonds, and the 1638 cm^{-1} peak represents C═C bonds. Also indicated are the peaks relative to the characteristic bonds that represent the PVDF α and β crystalline phases.

The results from ATR-FTIR measurements can also be used to confirm the crystalline phase of the membrane. The mechanical strength properties of the membranes can be influenced by its crystalline phase.[37,52] The characteristic absorption bands at 410, 531, 615, 764, 796, 855, and 976 cm^{-1} represent the α crystalline phase, while the β phase is identified by the bands at 442, 468, 510, and 840 cm^{-1}.[1,52−55] As shown in Figure 2, the γ-phase characteristic peaks at 776, 812, and 833 cm^{-1} were not observed for the samples prepared in this study,[52,54] while all of the membranes contained α and β PVDF crystalline phases. The 765 cm^{-1} band of PVDF2 and PVDF3 was more obvious than that of PVDF1 and PVDF4 membranes. The formation of α and β phases may be influenced by the temperature.[54] The α phase resulting from melting crystallization can be easily obtained at any temperature, while the 840 cm^{-1} band is common for both β and γ phases; when the temperature of solution crystallization is under 70 °C, the polymer solidification results in the β phase rather than the γ phase.[54]

3.3. Membrane Morphology. Micrographs of surface and cross-sectional morphologies were acquired using SEM, and representative images are shown in Figure 3. Using DMSO only as a solvent resulted in a surface with large pore sizes and irregular pore distribution. Therefore, total substitution of traditional solvents with DMSO was not a successful attempt, which may lead to defects on the membrane surface. After mixing DMSO with a certain percentage of traditional solvents, the pore size significantly decreased. Table 3 lists the main structural parameters of the fabricated membranes. PVDF/PVDF-*g*-PEGMA membranes synthesized in previous studies had pore size parameters, D_{avg} and D_{max}, of about 34 and 126 nm when using DMF/THF as the solvent mixture and 42 and 146 nm when using NMP as the solvent (Table 2).[28,30,31] In this study, the partial substitution of NMP and DMF/THF using DMSO translated in a significant pore shrinkage such that the pores could not be observed under 10k× or 100k× magnification on the surface of PVDF3 and PVDF4 membranes.[28] Relative to the cross-sectional morphologies, a top dense layer and an asymmetric structure were observed in all of the PVDF/PVDF-*g*-PEGMA membranes, with underlying porous fingerlike structures (PVDF1, PVDF3, and PVDF4) or macrovoids (PVDF2). The thickness of the membranes largely decreased when compared to that of

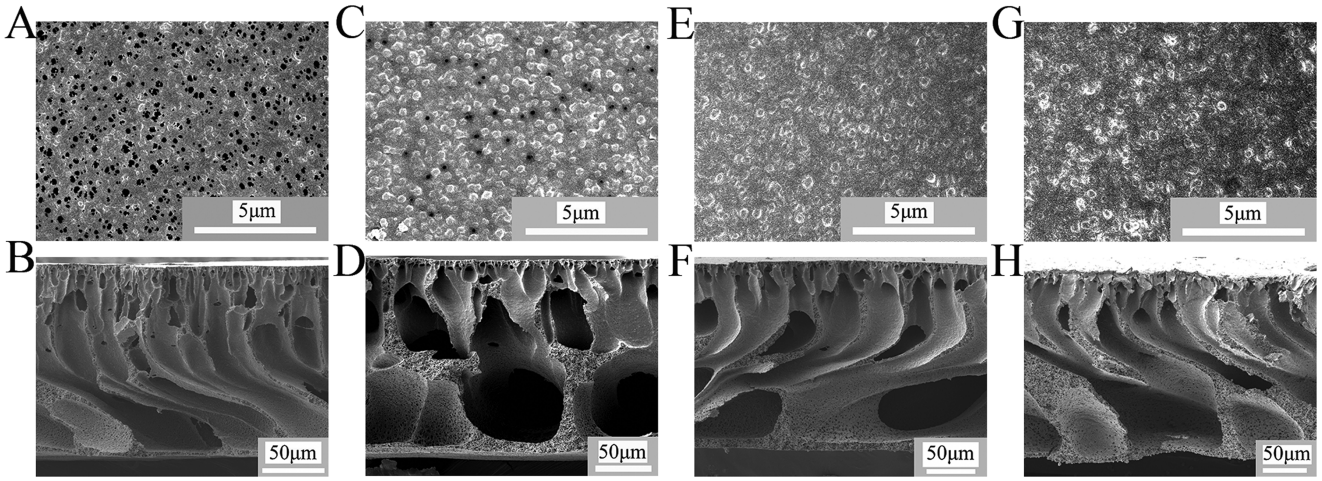

Figure 3. Representative SEM micrographs of the surface and cross-section morphologies of all of the PVDF/PVDF-*g*-PEGMA membranes. PVDF1, DMSO (A, B); PVDF2, DMSO/DMAc = 3:7 (C, D); PVDF3, NMP/DMSO = 5:5 (E, F); and PVDF4, THF/DMF/DMSO = 1.5:3.5:5 (G, H). The membrane surface images are shown in the top row, while the cross-sectional morphologies are shown in the bottom row.

DOI: 10.1021/acsomega.9b02674
ACS Omega 2019, 4, 19799−19807

Table 3. Properties of the PVDF/PVDF-*g*-PEGMA Ultrafiltration Membranes Fabricated in This Study

membrane ID	D_{avg} (nm)	D_{max} (nm)	thickness (μm)	SA rejection (%)	flux recovery (%)	permeability (L m^{-2} h^{-1} bar^{-1})	roughness (μm)	tensile strength (MPa)
PVDF1	111.02	519.09	155 ± 0.6	46.27 ± 4.18	29.16	214 ± 8	44.1 ± 0.4	1.04
PVDF2	46.47	185.91	173 ± 1.5	87.00 ± 2.41	89.33	735 ± 74	57.5 ± 6.1	0.88
PVDF3[a]			190 ± 2.3	81.21 ± 1.96	86.57	460 ± 27	54.7 ± 3.3	0.34
PVDF4[a]			216. ± 4.6	81.74 ± 3.33	86.38	532 ± 16	51.1 ± 5.9	1.04

[a]The pore sizes of PVDF3 and PVDF4 are very small that cannot be calculated by the SEM image.

PVDF/PVDF-*g*-PEGMA membranes synthesized in previous studies (Table 2), which was mainly due to the lower percentage of PVDF-*g*-PEGMA and PVDF in the casting solution. This mechanism led to a clear decrease in the mechanical strength, which was observed while handling the samples. The cross-sectional morphologies and the pore size distribution influence pure water flux, fouling, and flux recovery performance of the membrane,[37] which are discussed below.

3.4. Wettability. The wettability of the PVDF/PVDF-*g*-PEGMA membranes was estimated through sessile drop contact angle measurements. The results are reported in Figure 4. The initial contact angles were in the same range 65−70° as our previous study, whose results are reported in Table 2. However, the changes in the contact angle of our previous membranes were small (less than 10°) in 3 min. In contrast, for the membranes fabricated in this study, the contact angle reduction as a function of time was significant, especially for PVDF2. Specifically, the contact angles decreased from 63.8 ± 2.5 to 46.1 ± 4.9° in 18 s for PVDF1, from 70.8 ± 3.8 to 7.4 ± 1.4° for PVDF2, from 69.7 ± 3.9 to 49.9 ± 4.0° for PVDF3, and from 61.0 ± 2.5 to 45.3 ± 4.9° for PVDF4, which indicated that the wettability of PVDF/PVDF-*g*-PEGMA membranes was significantly enhanced.[56]

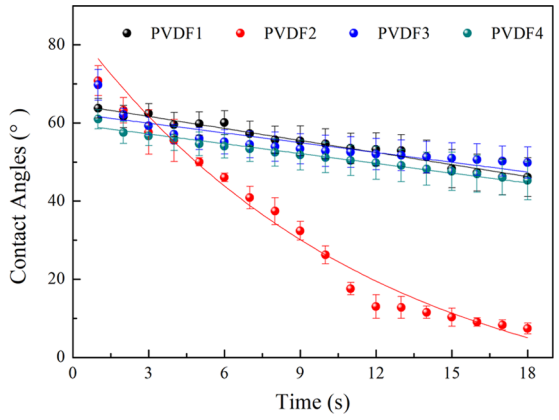

Figure 4. Contact angles as a function of time of PVDF/PVDF-*g*-PEGMA membranes using different solvents or solvent mixtures. PVDF1, DMSO; PVDF2, DMSO/DMAc = 7:3, PVDF3, DMSO/NMP = 5:5; and PVDF4, DMSO/THF/DMF = 5:1.5:3.5.

Many factors contribute to the wettability of the membrane, including the hydrophilic segments distribution, the surface roughness, and the surface pore size.[10] It has been reported that the air bubble/water droplet contact angle can be significantly affected by the surface roughness and solid surface heterogeneity.[57−59] According to the Wenzel model, a large quantity of surface amphiphilic or hydrophilic segments and a larger surface roughness will make the surface more hydrophilic. In this study, the enhancement in wettability is mainly attributed to the migration of a larger amount of PEGMA segments to the membrane surface, as well to the membrane morphology. In particular, the cross-sectional morphology observed for PVDF2 allowed faster spreading of water on this membrane. Wettability is important and may also enhance the antifouling properties of the membranes.

3.5. Surface Roughness. Representative AFM images of the fabricated PVDF/PVDF-*g*-PEGMA ultrafiltration membranes can be found in the SI (Figure S1), and their root mean square (RMS) surface roughness are shown in Table 3. The absolute RMS was within 60 nm. This value is larger than that of membranes fabricated in previous studies, which was about 15−30 nm. The reason is that the migration of PVDF-*g*-PEGMA segments to the surface can result in a larger RMS surface roughness, which is in accordance with the results reported by Liu et al. and Wang et al.[28,31] When using DMSO alone, the RMS roughness of the membrane was slightly lower than that of membranes fabricated by mixing traditional solvents with DMSO, showing that the solvent can also influence the membrane roughness. Usually, lower roughness translates into easier membrane cleaning and better antifouling properties.[60]

3.6. Membrane Transport and Antifouling Performance. The permeate flux of PVDF/PVDF-*g*-PEGMA membranes was recorded under a 0.07 MPa (10 psi) constant applied pressure. Figure 5 summarizes the flux profiles, the rejection rates of sodium alginate, and the fouling indices. The pure water permeabilities for PVDF1−PVDF4 were 214 ± 8 L, 735 ± 74, 460 ± 27, and 532 ± 16 L m^{-2} h^{-1} bar^{-1}, respectively. All of the membranes exhibited a sharp decline in flux during the filtration of an SA solution, with the flux reaching a near steady-state value of approximately 100 L m^{-2} h^{-1}. After physical cleaning for 1 min using pure water, the order of recovery fluxes for the four membranes was PVDF2 > PVDF3 > PVDF4 >PVDF1, which was similar to the order of highest to lowest water permeability. The different solvent or solvent mixture used in the casting dope had clearly a significant impact on flux, with variations above 300% for the membranes. Partial DMSO substitution achieved better results, with PVDF2 performing best possibly due to its better wettability and cross-sectional structure.

SA rejection rates are reported in Figure 5C. The size of the SA particle in the experiments was in the range of 15−80 nm; thus, SA particles can easily pass through the surface pores of PVDF1, leading to a low rejection rate. PVDF2 performed best, suggesting that wettability influenced the rejection and antifouling performance more than the surface pore size. Compared with membranes fabricated previously (Table 2), using DMSO decreased the SA rejection, which however was higher than 80% for the best membranes. The FRR, DR_t, DR_r, and DR_{ir} values of all PVDF/PVDF-*g*-PEGMA membranes are summarized in Figure 5B. High DR_r/DR_t and FRR indices are indicative of better antifouling properties, i.e., fouling reversibility, of the fabricated membranes.[61] The order of

DOI: 10.1021/acsomega.9b02674
ACS Omega 2019, 4, 19799−19807

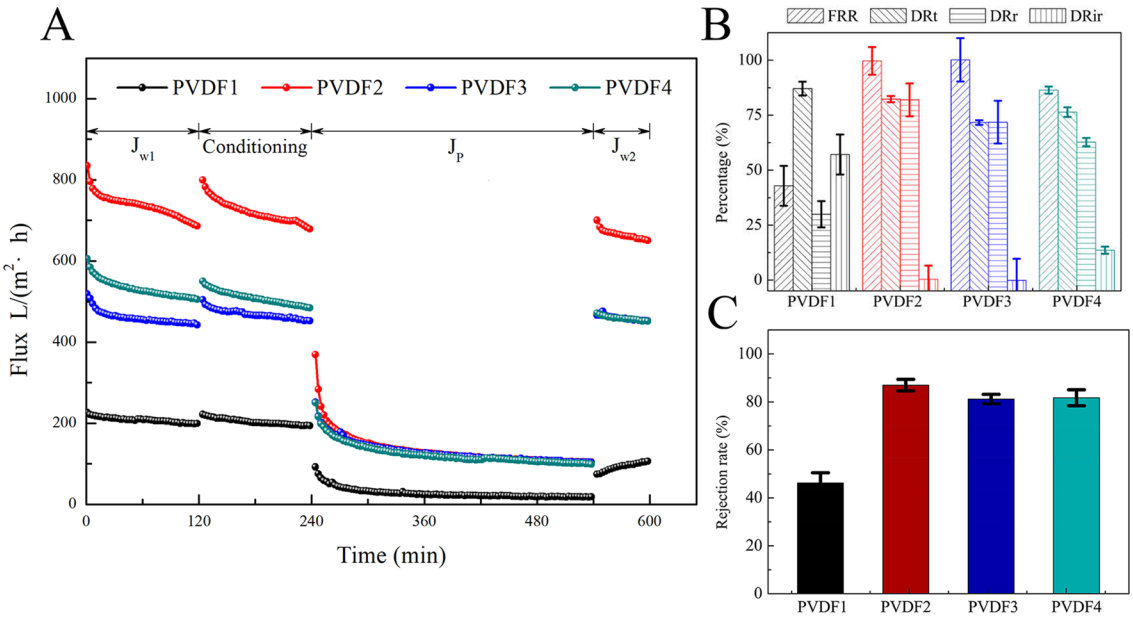

Figure 5. Transport performance and fouling behavior of the PVDF/PVDF-*g*-PEGMA membranes using different solvents or solvent mixtures. PVDF1, DMSO; PVDF2, DMSO/DMAc=3:7; PVDF3, DMSO/NMP=5:5; and PVDF4, DMSO/THF/DMF=5:1.5:3.5. (A) Flux as a function of time using pure water or sodium alginate as feed solution; B) FRR, DR_t, DR_r, and DR_{ir} indices; and (C) SA rejection.

FRR and DR_r/DR_t ratios was PVDF3 ∼ PVDF2 > PVDF4 ≫ PVDF1. Therefore, applying a partial substitution with green solvent DMSO produced an outstanding flux recovery rate in two cases. Despite the larger roughness of the membranes, the wettability, foulant rejection, and flux recovery ratios were beyond expectation. Therefore, we can conclude that hydrophilic segments on the surface of the membrane contribute more than the roughness to the fouling behavior of the membrane. In summary, performance of PVDF2 was outstanding, while the performance of PVDF1 was not satisfying, indicating that DMSO alone is not a good solvent for PVDF/PVDF-*g*-PEGMA fabrication under the tested conditions. However, using DMSO to partly substitute hazardous traditional solvents is a promising way to achieve a cleaner process as well as high-performance membranes.

4. CONCLUSIONS

Based on the calculation using the Hanson solubility theory, the total and partial substitution of hazardous traditional solvents with green solvent DMSO were investigated for the fabrication of PVDF membranes blended with PVDF-*g*-PEGMA. The total and partial substitution with DMSO generally improved the wettability and the fouling performance of the ultrafiltration membranes. Specifically, the membranes fabricated via partial substitution (PVDF2, 3, 4) performed better than the membrane fabricated from polymer solution of pure DMSO (PVDF1). The best performing membrane was cast from a solution containing DMAc and DMSO. This membrane had simultaneously high permeability of above 700 L m^{-2} h^{-1} bar^{-1}, high alginate rejection (87%), and showed remarkable antifouling performance with flux recovery rates of nearly 100%. According to the results of these experiments, the partial substitution of traditional organic solvents using green solvent DMSO to synthesize ultrafiltration membranes consisting of PVDF blended with PVDF-*g*-PEGMA can achieve a greener chemical process while also significantly enhancing the membrane performance.

■ ASSOCIATED CONTENT

Supporting Information

The Supporting Information is available free of charge on the ACS Publications website at DOI: 10.1021/acsomega.9b02674.

Calculations and experiment results; AFM morphologies of the fabricated membranes; mechanical performances of the fabricated membranes; calculation process using a group contribution method to calculate the solubility parameter of PEGMA; δ_d, δ_h, and δ_p values and densities of some solvents; detailed calculation of the δ_d, δ_h, and δ_p values of mixed solvents; FRR, DR_t, DR_r; and DR_{ir} results of the fabricated membranes (PDF)

■ AUTHOR INFORMATION

Corresponding Author

*E-mail: bcliu@scu.edu.cn, baicangliu@gmail.com. Tel: +86-28-85995998. Fax: +86-28-62138325.

ORCID

Alberto Tiraferri: 0000-0001-9859-1328

Baicang Liu: 0000-0003-3219-1924

Notes

The authors declare no competing financial interest.

■ ACKNOWLEDGMENTS

This work was supported by the National Natural Science Foundation of China (51678377), the State Key Laboratory of Separation Membranes and Membrane Processes (Tianjin Polytechnic University) (M2-201809), and the Fundamental Research Funds for the Central Universities. Alberto Tiraferri acknowledges the support from Politecnico di Torino. The authors thank Yi He at Analytical & Testing Center, Sichuan University for SEM measurements. The authors thank Sheng Chen and Yinghui Zhao at the College of Biomass Science and Engineering, Sichuan University for measurements of solution viscosity and membrane mechanical properties. The views and

DOI: 10.1021/acsomega.9b02674
ACS Omega 2019, 4, 19799−19807

ideas expressed herein are solely those of the authors and do not represent the ideas of the funding agencies in any form.

REFERENCES

(1) Buonomenna, M. G.; Lopez, L. C.; Favia, P.; d'Agostino, R.; Gordano, A.; Drioli, E. New PVDF membranes: The effect of plasma surface modification on retention in nanofiltration of aqueous solution containing organic compounds. *Water Res.* **2007**, *41*, 4309−4316.

(2) Chen, Y.; Deng, Q.; Mao, J.; Nie, H.; Wu, L.; Zhou, W.; Huang, B. Controlled grafting from poly(vinylidene fluoride) microfiltration membranes via reverse atom transfer radical polymerization and antifouling properties. *Polymer* **2007**, *48*, 7604−7613.

(3) Bonyadi, S.; Chung, T.-S. Highly porous and macrovoid-free PVDF hollow fiber membranes for membrane distillation by a solvent-dope solution co-extrusion approach. *J. Membr. Sci.* **2009**, *331*, 66−74.

(4) Boributh, S.; Chanachai, A.; Jiraratananon, R. Modification of PVDF membrane by chitosan solution for reducing protein fouling. *J. Membr. Sci.* **2009**, *342*, 97−104.

(5) Zheng, Z.-S.; Li, B.-B.; Duan, S.-Y.; Sun, D.; Peng, C.-K. Preparation of PVDF ultrafiltration membranes using PVA as pore surface hydrophilic modification agent with improved antifouling performance. *Polym. Eng. Sci.* **2019**, *59*, E384−E393.

(6) Sun, D.; Yue, D.; Li, B.; Zheng, Z.; Meng, X. Preparation and performance of the novel PVDF ultrafiltration membranes blending with PVA modified SiO2 hydrophilic nanoparticles. *Polym. Eng. Sci.* **2019**, *59*, E412−E421.

(7) Benhabiles, O.; Galiano, F.; Marino, T.; Mahmoudi, H.; Lounici, H.; Figoli, A. Preparation and Characterization of TiO2-PVDF/PMMA Blend Membranes Using an Alternative Non-Toxic Solvent for UF/MF and Photocatalytic Application. *Molecules* **2019**, *24*, No. 724.

(8) Wang, S.; Li, T.; Chen, C.; Chen, S.; Liu, B.; Crittenden, J. Non-woven PET fabric reinforced and enhanced the performance of ultrafiltration membranes composed of PVDF blended with PVDF-g-PEGMA for industrial applications. *Appl. Surf. Sci.* **2018**, *435*, 1072−1079.

(9) Venault, A.; Chang, C.-Y.; Tsai, T.-C.; Chang, H.-Y.; Bouyer, D.; Lee, K.-R.; Chang, Y. Surface zwitterionization of PVDF VIPS membranes for oil and water separation. *J. Membr. Sci.* **2018**, *563*, 54−64.

(10) Younas, H.; Bai, H.; Shao, J.; Han, Q.; Ling, Y.; He, Y. Super-hydrophilic and fouling resistant PVDF ultrafiltration membranes based on a facile prefabricated surface. *J. Membr. Sci.* **2017**, *541*, 529−540.

(11) Liu, C.; Wu, L.; Zhang, C.; Chen, W.; Luo, S. Surface hydrophilic modification of PVDF membranes by trace amounts of tannin and polyethyleneimine. *Appl. Surf. Sci.* **2018**, *457*, 695−704.

(12) Zeng, K.; Zhou, J.; Cui, Z.; Zhou, Y.; Shi, C.; Wang, X.; Zhou, L.; Ding, X.; Wang, Z.; Drioli, E. Insight into fouling behavior of poly(vinylidene fluoride) (PVDF) hollow fiber membranes caused by dextran with different pore size distributions. *Chin. J. Chem. Eng.* **2018**, *26*, 268−277.

(13) Jayalakshmi, A.; Rajesh, S.; Mohan, D. Fouling propensity and separation efficiency of epoxidated polyethersulfone incorporated cellulose acetate ultrafiltration membrane in the retention of proteins. *Appl. Surf. Sci.* **2012**, *258*, 9770−9781.

(14) Rajesh, S.; Jayalakshmi, A.; Senthilkumar, S.; Sankar, H. S. H.; Mohan, D. R. Performance Evaluation of Poly(amide-imide) Incorporated Cellulose Acetate Ultrafiltration Membranes in the Separation of Proteins and Its Fouling Propensity by AFM Imaging. *Ind. Eng. Chem. Res.* **2011**, *50*, 14016−14029.

(15) Behboudi, A.; Jafarzadeh, Y.; Yegani, R. Polyvinyl chloride/polycarbonate blend ultrafiltration membranes for water treatment. *J. Membr. Sci.* **2017**, *534*, 18−24.

(16) Ma, W.; Rajabzadeh, S.; Shaikh, A. R.; Kakihana, Y.; Sun, Y.; Matsuyama, H. Effect of type of poly(ethylene glycol) (PEG) based amphiphilic copolymer on antifouling properties of copolymer/poly(vinylidene fluoride) (PVDF) blend membranes. *J. Membr. Sci.* **2016**, *514*, 429−439.

(17) Hashim, N. A.; Liu, F.; Abed, M. R. M.; Li, K. Chemistry in spinning solutions: Surface modification of PVDF membranes during phase inversion. *J. Membr. Sci.* **2012**, *415*, 399−411.

(18) Wu, H.; Li, T.; Liu, B.; Chen, C.; Wang, S.; Crittenden, J. C. Blended PVC/PVC-g-PEGMA ultrafiltration membranes with enhanced performance and antifouling properties. *Appl. Surf. Sci.* **2018**, *455*, 987−996.

(19) Yang, B.; Yang, X.; Liu, B.; Chen, Z.; Chen, C.; Liang, S.; Chu, L.-Y.; Crittenden, J. PVDF blended PVDF-g-PMAA pH-responsive membrane: Effect of additives and solvents on membrane properties and performance. *J. Membr. Sci.* **2017**, *541*, 558−566.

(20) Hester, J. F.; Banerjee, P.; Won, Y. Y.; Akthakul, A.; Acar, M. H.; Mayes, A. M. ATRP of amphiphilic graft copolymers based on PVDF and their use as membrane additives. *Macromolecules* **2002**, *35*, 7652−7661.

(21) Ran, J.; Wu, L.; Zhang, Z.; Xu, T. Atom transfer radical polymerization (ATRP): A versatile and forceful tool for functional membranes. *Prog. Polym. Sci.* **2014**, *39*, 124−144.

(22) Xu, F. J.; Zhao, J. P.; Kang, E. T.; Neoh, K. G.; Li, J. Functionalization of nylon membranes via surface-initiated atom-transfer radical polymerization. *Langmuir* **2007**, *23*, 8585−8592.

(23) Zhou, Z.; Rajabzadeh, S.; Shaikh, A. R.; Kakihana, Y.; Ma, W.; Matsuyama, H. Effect of surface properties on antifouling performance of poly(vinyl chloride-co-poly(ethylene glycol)methyl ether methacrylate)/PVC blend membrane. *J. Membr. Sci.* **2016**, *514*, 537−546.

(24) Matyjaszewski, K. Advanced Materials by Atom Transfer Radical Polymerization. *Adv. Mater.* **2018**, *30*, No. 1706441.

(25) Matyjaszewski, K. Atom Transfer Radical Polymerization (ATRP): Current Status and Future Perspectives. *Macromolecules* **2012**, *45*, 4015−4039.

(26) Bhattacharya, A.; Misra, B. N. Grafting: a versatile means to modify polymers - Techniques, factors and applications. *Prog. Polym. Sci.* **2004**, *29*, 767−814.

(27) Chang, Y.; Ko, C.-Y.; Shih, Y.-J.; Quemener, D.; Deratani, A.; Wei, T.-C.; Wang, D.-M.; Lai, J.-Y. Surface grafting control of PEGylated poly(vinylidene fluoride) antifouling membrane via surface-initiated radical graft copolymerization. *J. Membr. Sci.* **2009**, *345*, 160−169.

(28) Liu, B.; Chen, C.; Li, T.; Crittenden, J.; Chen, Y. High performance ultrafiltration membrane composed of PVDF blended with its derivative copolymer PVDF-g-PEGMA. *J. Membr. Sci.* **2013**, *445*, 66−75.

(29) Hashim, N. A.; Liu, F.; Li, K. A simplified method for preparation of hydrophilic PVDF membranes from an amphiphilic graft copolymer. *J. Membr. Sci.* **2009**, *345*, 134−141.

(30) Chen, C.; Tang, L.; Liu, B.; Zhang, X.; Crittenden, J.; Chen, K. L.; Chen, Y. Forming mechanism study of unique pillar-like and defect-free PVDF ultrafiltration membranes with high flux. *J. Membr. Sci.* **2015**, *487*, 1−11.

(31) Wang, S.; Li, T.; Chen, C.; Liu, B.; Crittenden, J. C. PVDF ultrafiltration membranes of controlled performance via blending PVDF-g-PEGMA copolymer synthesized under different reaction times. *Front. Environ. Sci. Eng.* **2018**, *12*, 3.

(32) Sheldon, R. A. Metrics of Green Chemistry and Sustainability: Past, Present, and Future. *ACS Sustainable Chem. Eng.* **2018**, *6*, 32−48.

(33) Giraud, R. J.; Williams, P. A.; Sehgal, A.; Ponnusamy, E.; Phillips, A. K.; Manley, J. B. Implementing Green Chemistry in Chemical Manufacturing: A Survey Report. *ACS Sustainable Chem. Eng.* **2014**, *2*, 2237−2242.

(34) Clarke, C. J.; Tu, W. C.; Levers, O.; Brohl, A.; Hallett, J. P. Green and Sustainable Solvents in Chemical Processes. *Chem. Rev.* **2018**, *118*, 747−800.

(35) Sheldon, R. A. The E factor 25 years on: the rise of green chemistry and sustainability. *Green Chem.* **2017**, *19*, 18−43.

DOI: 10.1021/acsomega.9b02674
ACS Omega 2019, 4, 19799−19807

(36) Gałuszka, A.; Migaszewski, Z.; Namiesnik, J. The 12 principles of green analytical chemistry and the SIGNIFICANCE mnemonic of green analytical practices. *TrAC, Trends Anal. Chem.* **2013**, *50*, 78−84.
(37) Liu, F.; Hashim, N. A.; Liu, Y.; Abed, M. R. M.; Li, K. Progress in the production and modification of PVDF membranes. *J. Membr. Sci.* **2011**, *375*, 1−27.
(38) Yeow, M. L.; Liu, Y. T.; Li, K. Morphological study of poly(vinylidene fluoride) asymmetric membranes: Effects of the solvent, additive, and dope temperature. *J. Appl. Polym. Sci.* **2004**, *92*, 1782−1789.
(39) Ali, I.; Bamaga, O. A.; Gzara, L.; Bassyouni, M.; Abdel-Aziz, M. H.; Soliman, M. F.; Drioli, E.; Albeirutty, M. Assessment of Blend PVDF Membranes, and the Effect of Polymer Concentration and Blend Composition. *Membranes* **2018**, *8*, 13.
(40) Marino, T.; Galiano, F.; Simone, S.; Figoli, A. DMSO EVOL as novel non-toxic solvent for polyethersulfone membrane preparation. *Environ. Sci. Pollut. Res.* **2019**, *26*, 14774−14785.
(41) Wang, H. H.; Jung, J. T.; Kim, J. F.; Kim, S.; Drioli, E.; Lee, Y. M. A novel green solvent alternative for polymeric membrane preparation via nonsolvent-induced phase separation (NIPS). *J. Membr. Sci.* **2019**, *574*, 44−54.
(42) Arahman, N.; Mulyati, S.; Fahrina, A. Morphology and performance of pvdf membranes composed of triethylphospate and dimethyl sulfoxide solvents. *Mater. Res. Express* **2019**, *6*, No. 066419.
(43) Evenepoel, N.; Wen, S.; Tsehaye, M. T.; Van der Bruggen, B. Van der Bruggen, B. Potential of DMSO as greener solvent for PES ultra- and nanofiltration membrane preparation. *J. Appl. Polym. Sci.* **2018**, *135*, No. 46494.
(44) Xie, W.; Li, T.; Chen, C.; Wu, H.; Liang, S.; Chang, H.; Liu, B.; Drioli, E.; Wang, Q.; Crittenden, J. C. Using the Green Solvent Dimethyl Sulfoxide To Replace Traditional Solvents Partly and Fabricating PVC/PVC-g-PEGMA Blended Ultrafiltration Membranes with High Permeability and Rejection. *Ind. Eng. Chem. Res.* **2019**, *58*, 6413−6423.
(45) Bottino, A.; Capannelli, G.; Munari, S.; Turturro, A. Solubility Parameters of Poly(vinylidene fluoride). *J. Polym. Sci., Part B: Polym. Phys.* **1988**, *26*, 785−794.
(46) Van Krevelen, D. W.; Te Nijenhuis, K. Cohesive Properties and Solubility. In *Properties of Polymers*, 4th ed.; Elsevier: Amsterdam, 2009; Chapter 7, pp 189−227.
(47) Liu, B.; Chen, C.; Zhang, W.; Crittenden, J.; Chen, Y. Low-cost antifouling PVC ultrafiltration membrane fabrication with Pluronic F 127: Effect of additives on properties and performance. *Desalination* **2012**, *307*, 26−33.
(48) Asatekin, A.; Kang, S.; Elimelech, M.; Mayes, A. M. Anti-fouling ultrafiltration membranes containing polyacrylonitrile-graft-poly (ethylene oxide) comb copolymer additives. *J. Membr. Sci.* **2007**, *298*, 136−146.
(49) Zhao, X.; Su, Y.; Li, Y.; Zhang, R.; Zhao, J.; Jiang, Z. Engineering amphiphilic membrane surfaces based on PEO and PDMS segments for improved antifouling performances. *J. Membr. Sci.* **2014**, *450*, 111−123.
(50) Zhao, X.; Su, Y.; Chen, W.; Peng, J.; Jiang, Z. Grafting perfluoroalkyl groups onto polyacrylonitrile membrane surface for improved fouling release property. *J. Membr. Sci.* **2012**, *415*, 824−834.
(51) Chen, Y. W.; Liu, D. M.; Deng, Q. L.; He, X. H.; Wang, X. F. Atom transfer radical polymerization directly from poly(vinylidene fluoride): Surface and antifouling properties. *J. Polym. Sci., Part A: Polym. Chem.* **2006**, *44*, 3434−3443.
(52) Benz, M.; Euler, W. B. Determination of the crystalline phases of poly(vinylidene fluoride) under different preparation conditions using differential scanning calorimetry and infrared spectroscopy. *J. Appl. Polym. Sci.* **2003**, *89*, 1093−1100.
(53) Sencadas, V.; Gregorio, R.; Lanceros-Mendez, S. Processing and characterization of a novel nonporous poly(vinilidene fluoride) films in the beta phase. *J. Non-Cryst. Solids* **2006**, *352*, 2226−2229.
(54) Gregorio, R. Determination of the alpha, beta, and gamma crystalline phases of poly(vinylidene fluoride) films prepared at different conditions. *J. Appl. Polym. Sci.* **2006**, *100*, 3272−3279.
(55) Chang, H.; Li, T.; Liu, B.; Chen, C.; He, Q.; Crittenden, J. C. Smart ultrafiltration membrane fouling control as desalination pretreatment of shale gas fracturing wastewater: The effects of backwash water. *Environ. Int.* **2019**, *130*, 104869.
(56) Shen, J.; Zhang, Q.; Yin, Q.; Cui, Z.; Li, W.; Xing, W. Fabrication and characterization of amphiphilic PVDF copolymer ultrafiltration membrane with high anti-fouling property. *J. Membr. Sci.* **2017**, *521*, 95−103.
(57) Vogler, E. A. Structure and reactivity of water at biomaterial surfaces. *Adv. Colloid Interface Sci.* **1998**, *74*, 69−117.
(58) Tang, K.; Wang, X.; Yan, W.; Yu, J.; Xu, R. Fabrication of superhydrophilic Cu2O and CuO membranes. *J. Membr. Sci.* **2006**, *286*, 279−284.
(59) Yuan, J.; Liu, X.; Akbulut, O.; Hu, J.; Suib, S. L.; Kong, J.; Stellacci, F. Superwetting nanowire membranes for selective absorption. *Nat. Nanotechnol.* **2008**, *3*, 332−336.
(60) Akthakul, A.; Salinaro, R. F.; Mayes, A. M. Antifouling polymer membranes with subnanometer size selectivity. *Macromolecules* **2004**, *37*, 7663−7668.
(61) Xu, Z.; Liao, J.; Tang, H.; Efome, J. E.; Li, N. Preparation and antifouling property improvement of Troger's base polymer ultrafiltration membrane. *J. Membr. Sci.* **2018**, *561*, 59−68.

DOI: 10.1021/acsomega.9b02674
ACS Omega 2019, 4, 19799−19807